Asian Journal of Chemistry; Vol. 25, No. 17 (2013), 9605-9609

ASIAN JOURNAL OF CHEMISTRY

http://dx.doi.org/10.14233/ajchem.2013.15094

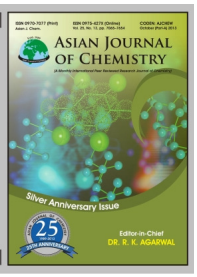

Polyol Mediated Synthesis and Microstructural Features of Polycrystalline $LiMPO_4$ (M = Mn and Co) Olivine Phosphates for Lithium Batteries

N. PADMANATHAN* and S. SELLADURAI

Ionics Lab, Department of Physics, Anna University, Chennai-600 025, India

*Corresponding author: Tel: +91 44 22358679; E-mail: padmanmsc@gmail.com

(*Received*: 4 January 2013; *Accepted*: 7 October 2013) AJC-14237

Well crystalline $LiMPO_4$ (M = Mn and Co) powder was synthesized *via* polyol mediated wet chemical route at low temperature. Glutinous diethylene glycol plays an important role during synthesis which provide reducing atmosphere, lessen the surplus agglomeration and hinders the particle growth. The phase and micro-structural features of the obtained olivine phosphate was analyzed by powder X-ray diffraction, scanning electron microscope and transmission electron microscope. X-ray diffraction analysis demonstrates that the sample exhibits pure orthorhombic structure with Pnma space group. Morphological scrutiny flaunts the formation of uniformly distributed nanosize particles appeared spherical in shape. The statistical mean diameter of the particles was approximately at 200 nm for $LiMPO_4$ nanostructures. As prepared olivine micro/nanostructure can be more favorable for fast lithium insertion/extraction reaction. Using the proposed polyol technique, it is possible to obtain the well crystalline submicron and nano size olivine phosphates for high potential lithium battery applications.

Key Words: Olivine, Polyol method, Glutinous diethylene glycol, Lithium ion batteries.

INTRODUCTION

The demands on high energy batteries in electronic devices have received considerable interest to the investigation of new kind of effective electrode materials suitable for modern portable devices such as laptops, cell phones, video camera and hybrid vehicles[1]. Currently lithium based transition metal oxide materials with layered structure are being used in lithium secondary batteries. The development of new alternative cathode materials to replace the present conventional system used in commercial rechargeable batteries has given new platform in battery research. At present most successful positive electrode materials of the conventional lithium secondary batteries are $LiMO_2$ (M = Mn, Co and Ni) and their layered structure offers considerably large number of lithium ion diffusion[2]. However, the major drawbacks on transition metal oxide cathode materials are their high cost, environmental hazard and poor electrochemical stability during the oxidation in large scale application which arouse researcher to find alternate cathode material for high energy application[2-5]. Of the various material studied, the olivine phosphates $LiMPO_4$ (M = Mn, Fe, Co and Ni) are found to be a suitable cathode materials with smart electrochemical properties[6].

In recent years, many research groups have investigated vastly the olivine phosphates $LiMPO_4$ (M = Mn, Fe, Co and Ni) as the next generation cathode material for lithium ion batteries[6-8]. Among these different olivine's, $LiFePO_4$ is widely studied since its introduction in 1997 as most favorable cathode for Li-ion secondary batteries. Due to their better performance (working voltage 3.5 V), easy synthesis and high stability in common organic electrolyte it has been largely investigated[9-11]. Although with the above advantages $LiFePO_4$ has certain critical and hampering issues such as micron size particles, poor electronic conductivity, less lithium ion diffusion and low working voltage, limits their application in high power batteries[12]. In order to increase lithium ion diffusion, intrinsically the lithium vacancy has been created by delithiation process. To improve their electrochemical performance and stability, novel synthesis procedures should developed. Therefore, various synthesis methods have been adopted to prepare nanosized electrode material with high crystallinity[5].

In the above aspects, investigation of $LiFePO_4$ has been achieved at the commercial level of rate capability and cyclability. However, still it shows relatively low potential (3.5 V) which cause a major impediment to its application. But the commercial need of high power batteries and the limitations of $LiFePO_4$ induced strong interest toward the other members of $LiMPO_4$, especially $LiMnPO_4$ and $LiCoPO_4$ due to their high theoretical energy density running up to above 800 Wh/kg based on its inherently high Mn^{2+}/Mn^{3+} and Co^{3+}/Co^{2+} redox

potentials of 4.2 and 4.8 V, respectively *versus* Li/Li^{+}[13,14]. As similar to $LiFePO_4$ the other olivine materials also provide better electrochemical performance. However, due to the difficult synthetic conditions of the $LiMnPO_4$ and $LiCoPO_4$, only limited number of results was reported elsewhere with the other olivine family as the cathode material for lithium batteries. In this work, $LiMPO_4$ (M = Mn and Co) which are belong to the olivine family has been synthesized through the inventive polyol process using diethylene glycol. Further, the structural features of the $LiCoPO_4$ and $LiMnPO_4$ nanoparticles were investigated.

EXPERIMENTAL

Synthesis procedure: Olivine structured $LiMPO_4$ nanoparticles with Mn and Co metals were synthesized by the procedure as reported by Wang *et al.*[15]; with slight modifications. The schematic diagram of the synthetic procedures is shown in Fig. 1. All reagents used in the experiments were purchased from the Alfa Aaser in analytical grade and used as received without further purifications. Initially, the stoichiometric amount of respective metal acetates $M(OOCCH_3)_2{\cdot}4H_2O$ (M = Mn and Co) were dissolved in deionized water. 100 mL of diethylene glycol (Merck Germany 99 %) was added to the solutions and stirred for 15 min. The highly viscous diethylene glycol protects the oxidation and minimizes the agglomeration of the particle. The obtained polyol mediated solutions were kept at 140 ºC for 1 h in the heating mantle. During this preheating time the stoichiometric amount of LiH_2PO_4 dissolved in deionized water under stirring then it was dropped into polyol mixed solution over the period of 15 min. The solution was replaced to double neck round bottom flask attached with reflux condenser. Diethylene glycol mixed solution was rapidly heated to 190 ºC and maintained at the same temperature for another 6 h under reflux. The pH of the solution was vigilantly monitored and maintain at 9 by adding the ammonia solution. The solution was cooled down to room temperature and kept in dark for further 24 h for completion of the nucleation. Finally, the precipitated materials were estranged and washed several times with deionized water, ethanol and acetone through continual centrifugation in order to confiscate the residual solvent and superfluous impurities. The ensuing products were desiccated at 120 ºC for overnight and annealed at 600 ºC for 6 h in air atmosphere.

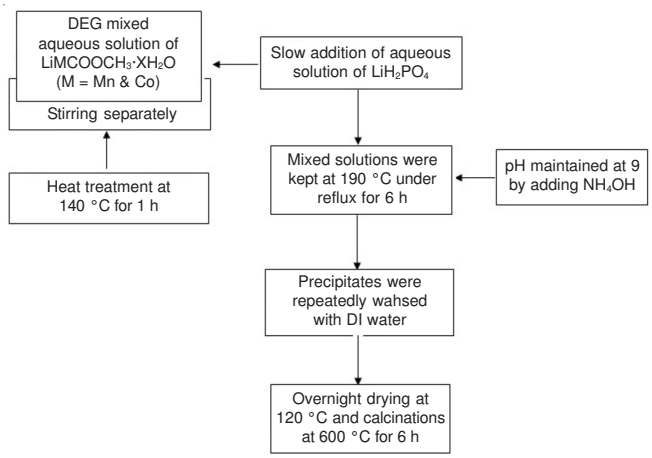

Fig. 1. Schematic descriptions of typical polyol synthesis process

Characterization method: X-Ray diffraction pattern was performed by Bruker D2 Phaser powder diffractometer using CuK_α radiation of wavelength 1.5406 Å with corresponding 2θ = 10-80º at a step size of 0.02º with 0.05 s count rate. Thermal decomposition of the material was studied by Thermo Gravimetric Analyzer (Bruker SDT Q600) under N_2 atmosphere at 10 ºC/min temperature range over 30-1000 ºC. Local cationic distribution and chemical structure of the synthesized material was analyzed using FTIR Spectroscopy (Spec Horiba Jobin Yvon spectrofluorimeter (F-311)). TEM images of the sample were monitored by FEI Tecnai T20 G2 (FEG) transmission electron microscope. The sample was gold coated before examined the morphology using LEO 1530 scanning electron microscope (SEM) instrument equipped with an energy dispersive X-ray spectroscopy (EDS) attachment. Images were recorded at 15 kV with a secondary electron detector. The Raman spectrum was recorded by Bruker Dispersive Laser Raman spectrophotometer using a pulsed He-Ne laser with the excitation wavelength of 532 nm as the radiation source; 25 % of the total power (40 mW) was employed for the measurements.

RESULTS AND DISCUSSION

Thermal analysis: The crystallization temperature of the olivine phosphates were confirmed initially by the thermogravimetric analysis. Fig. 2 shows the TGA curves of $LiMPO_4$ (M = Mn and Co) over the temperature range of 30-1000 ºC. Both the samples were showed the similar TGA curve which concludes that the crystallization of the Mn and Co cations followed the same chemical reaction. In TGA curve the initial weight loss obtained below 200 ºC is attributed to the removal of water and diethylene glycol from the compound mixture. The maximum weight loss occurred in the temperature range 200-400 ºC implies the decomposition of all the material precursors such as LiH_2PO_4 and the corresponding M^{2+} transition metal acetates. The continuous weight loss recorded at 400-600 ºC assigned to the process of nucleation and crystallization. Since beyond 600 ºC no weight loss has been found, which concludes the formation of well crystallized and phase pure $LiMPO_4$ above 600 ºC. Modified polyol synthesis process considerably decreases the crystallization temperature compared to the earlier ceramic and wet chemical synthesis process.

Structural analysis: The XRD pattern of $LiMPO_4$ (M = Mn and Co) are shown in Fig. 3 indicates the material are well belongs to the olivine phase orthorhombic structure with Pnma space group. The superior and razor-sharp intensity peaks without any misfits due to $LiPO_4$, exemplified the presence of pure crystals with single phase functional compounds was achieved by adopted polyol method. The lattice parameters and the average particle size of the samples are shown in Table-1 which index the synthesized samples are having very good agreement with the respective standard JCPDS files that are PDF # 77-0178 and PDF # 32-0552 for $LiMnPO_4$ and $LiCoPO_4$, respectively. The particle size of the prepared olivine lithium metal phosphates were calculated using Scherrer equation:

$$d = \frac{0.9\lambda}{\beta_{1/2}\cos\theta}$$

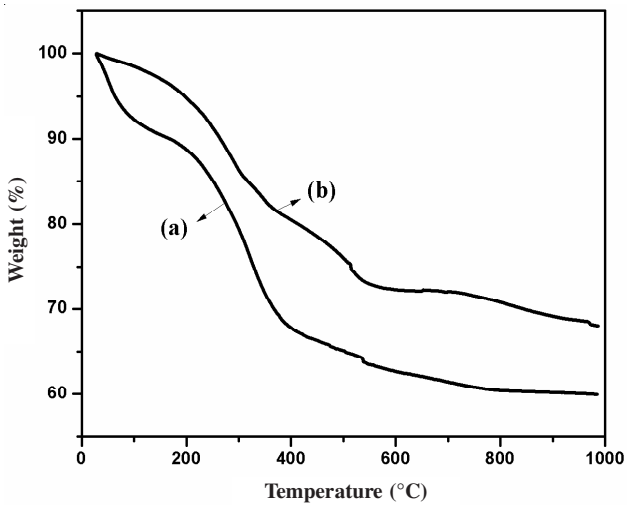

Fig. 2. TGA curves of $LiMnPO_4$ (a) and $LiCoPO_4$ (b)

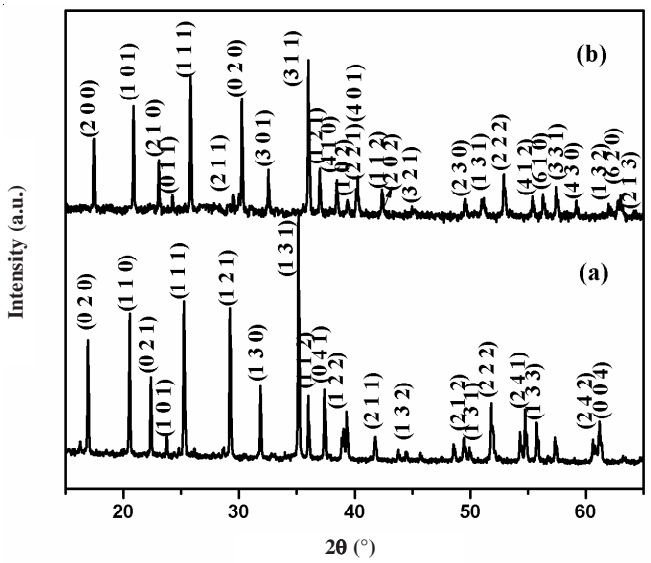

Fig. 3. XRD pattern of polyol synthesized $LiMnPO_4$ (a) and $LiCoPO_4$ (b)

TABLE-1
LATTICE PARAMETERS OF $LiMPO_4$ (M = Mn AND Co) NANOSTRUCTURE SYNTHESIZED *VIA* POLYOL METHOD

Compound name	Lattice parameters in (Å)			Cell volume in (Å^3)	Average crystallite size in (nm)
	a	b	c		
$LiMnPO_4$ JCPDS-77-0178	4.694	10.330	6.041	294.96	64
$LiCoPO_4$ JCPDS-32-0552	5.912	10.191	4.693	284.15	58

where λ = X-rays wavelength, θ = diffraction angle, $\beta_{1/2}$ = full width half maximum value.

XRD investigation concludes the polyol based synthesis process offer a high crystalline and single phase $LiMPO_4$ nanoparticles with orthorhombic structure as active material for cathode applications. Typical structural configuration of olivine $LiMnPO_4$ and their strong covalent PO_4 units make the momentous potential for high energy secondary lithium batteries.

FTIR and Raman studies: Fig. 4 shows the FTIR spectra of $LiMPO_4$ (M = Mn and Co) phospho-olivine material which confirms the chemical structure of the functional material. The structural edifice of olivine phase material arranged in the order of LiO_6 and MO_6 octahedra bonded with strong PO_4^{3-} polyanion[14,16,17]. Generally, the internal vibrations of $LiMPO_4$ were conquered by the fundamental modes ν_1-ν_4 of polyanion. The observed FTIR spectra shows three broadly distributed peaks around 1050, 600 and 450 cm^{-1} which corresponds to stretching and bending vibrational modes of tetrahedral PO_4^{3-} molecules. The assymmetric stretching vibration modes of PO_4^{3-} appeared at 977 cm^{-1} (ν_1), the doublet peak present at 470 cm^{-1} (ν_2) and the triplet peaks displayed at 1150-980 cm^{-1} (ν_3) and 637-580 cm^{-1} (ν_4). These PO_4^{3-} vibrational modes splitting may be endorsed to coupling of corresponding transition metal oxide bonding in the structure which confirms the formation of pure $LiMPO_4$ compounds[16]. The intramolecular vibrational spectra of phospho-olivine sample calcined at 600 ºC was obtained by Dispersive Laser Raman Spectrophotometer, the corresponding fundamental modes of PO_4^{3-} polyanion complements with FTIR spectra which occur in the region 600-1000 cm^{-1}. The observed Raman spectrum is shown in Fig. 5. When compared to $LiMnPO_4$, the Raman stretching mode intensity (ν_4) increased for $LiCoPO_4$ which confronts the appearance of strong covalent bond between Co^{2+} and corresponding polyanion[16,18].

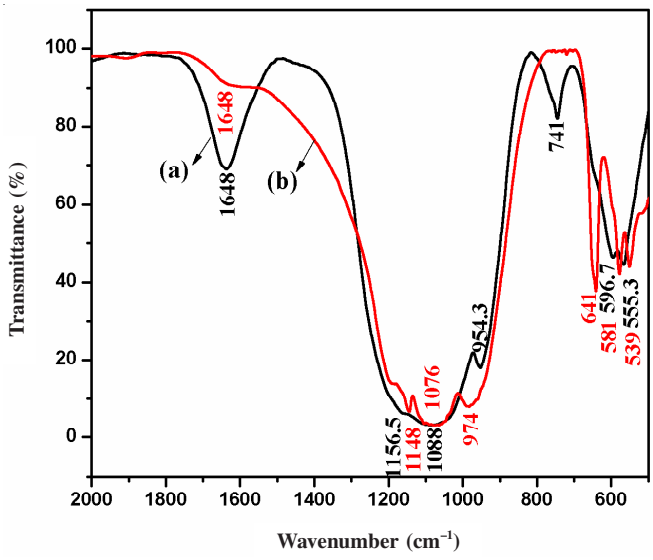

Fig. 4. FTIR spectra of $LiMnPO_4$ (a) and $LiCoPO_4$ (b) nanostructure synthesized using diethylene glycol

Morphological and microstructure analysis: SEM and TEM pictures were taken in order to identify the surface morphology, microstructure and actual crystallite size of the synthesized $LiMPO_4$ compounds. The SEM micrographs with different magnifications are shown in Fig. 6(a-f). This clearly monitored the submicron size particles are well-dispersed and slightly agglomerated. The observed similes apparently reflect the particles were uniformly distributed with rod and spherical surface morphology for $LiMnPO_4$ and $LiCoPO_4$, respectively. For further evidences the TEM descriptions are shown in Fig. 7(a-d). The geometric mean particle diameter was measured at around 50-65 nm. In Fig. 7(e and f) the observed selected area electron diffraction (SAED) pattern shows the distinct and fine diffraction rings due to the respective planes of $LiMPO_4$

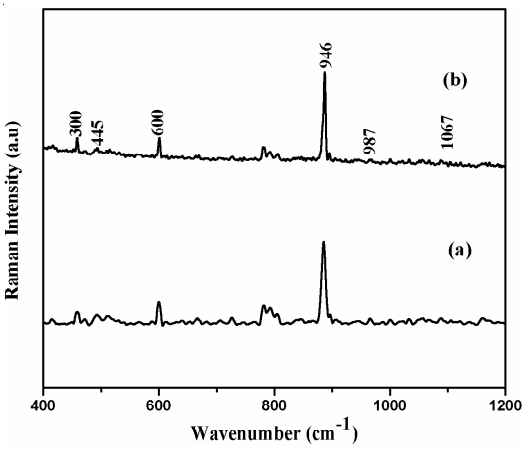

Fig. 5. Raman spectra of $LiMnPO_4$ (a) and $LiCoPO_4$ (b)

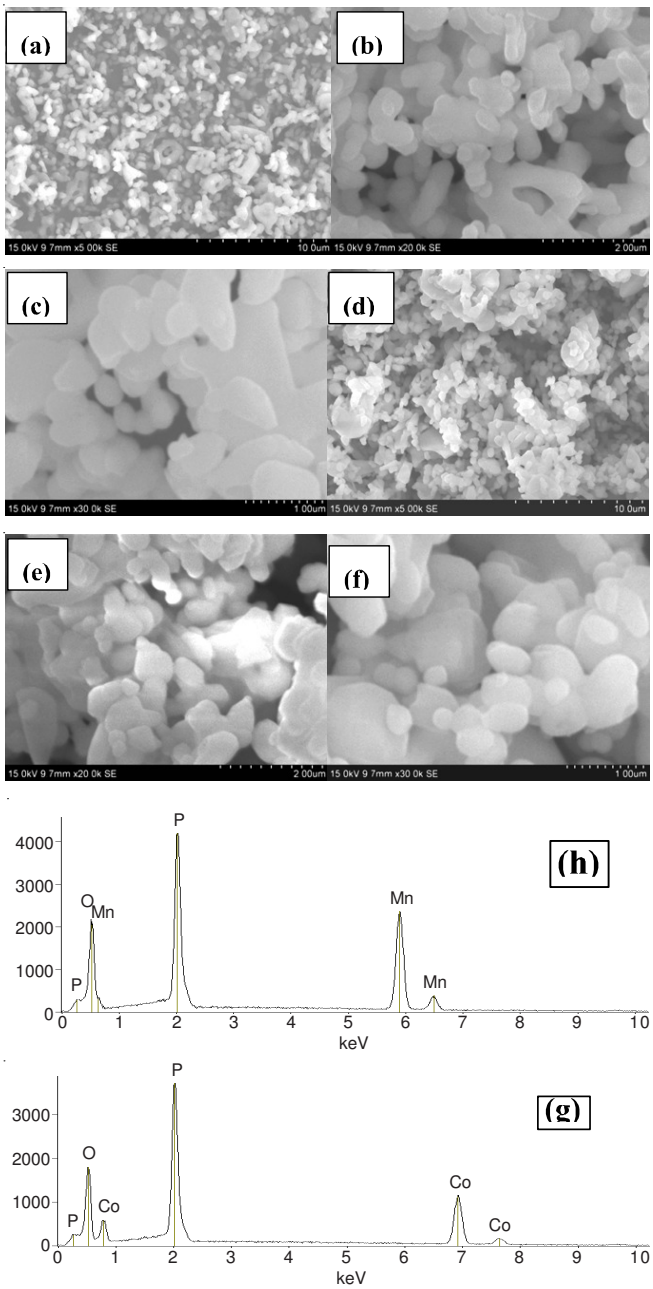

Fig. 6. (a-f) SEM images of $LiMPO_4$ [M = Mn (a, b, c & h) and Co (d, e, f & g)] with different magnifications and their corresponding EDS spectra (g and h)

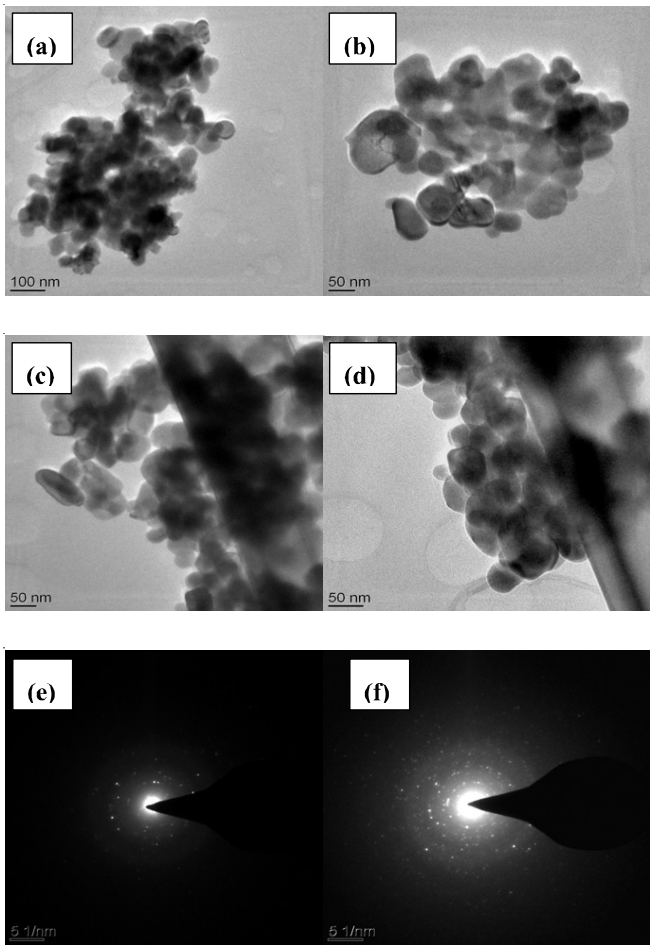

Fig. 7. (a-f) TEM images of $LiMPO_4$ [M = Mn (a, b & e) and Co (c, d & f)] at different magnifications with their corresponding SAED pattern

with the corresponding orthorhombic structure. The intensity of the rings obtained from the SAED indicates the particles are well crystalline and equally distributed. This kind of optimized surface morphology and nanosize particles are favourable for the lithium intercalation and de-intercalation process. Energy dispersive X-ray spectrum analysis (EDS) equipped with scanning electron microscope of $LiMPO_4$ samples are shown in Fig. 6g and h ascribes the presence of contributed elements in the compound. This further confirms the purity of the compounds with atomic stochiometry.

Conclusion

A single phase pristine $LiMPO_4$ (M = Mn and Co) nanoparticles were successfully synthesized *via* low temperature modified polyol route under reflux. The adopted method is found to be an effective way to prepare $LiMPO_4$ nanoparticles with desired size and morphology needed for electrochemical applications. XRD pattern confirm the synthesized cathode material belongs to the orthorhombic structure with Pnma space group. FTIR and Raman studies reveal that the local cation distribution and functional structure of the sample. SEM and TEM images confronts the agglomerated $LiMPO_4$ appeared in spherical morphology with an average particle size of 56 nm. Furthermore, the desired nanosize particle offers the advantage to achieve large number of lithium ion diffusion for high energy secondary battery applications.

ACKNOWLEDGEMENTS

The authors thank University Grant Commission, India, for the financial support.

REFERENCES

1. Y.P. Wu, C. Wan, C. Jiang and S.B. Fang, Lithium Ion Secondary Batteries, Chemical Industry Press, Beijing (2002).
2. J.M. Tarascon and M. Armand, *Nature*, **414**, 359 (2001).
3. J.R. Dahn, U. Von Sacken, M.W. Juzkow and H. Al-Janaby, *J. Electrochem. Soc*., **138**, 2207 (1991).
4. I.S. Jeong, J.U. Kim and H.B. Gu, *J. Power Sources*, **102**, 55 (2001).
5. H. Liu, Y.P. Wu, E. Rahm, R. Holze and H.Q. Wu, *J. Solid State Eletrochem*., **8**, 450 (2004).
6. A.K. Padhi, K.S. Nanjundaswamy, C. Masquelier, S. Okada and J.B. Goodenough, *J. Electrochem. Soc*., **144**, 1609 (1997).
7. F. Zhou, M. Cococcioni, K. Kang and G. Ceder, *Electrochem. Commun*., **6**, 1144 (2004).
8. D.-H. Seo, H. Gwon, S.-W. Kim, J. Kim and K. Kang, *Chem. Mater*., **22**, 518 (2010).
9. M. Gaberscek, R. Dominko and J. Jamnik, *Electrochem. Commun*., **9**, 2778 (2007).
10. Y.Q. Wang, J.L. Wang, J. Yang and Y.N. Nuli, *Adv. Funct. Mater*., **16**, 2135 (2006).
11. B. Ellis, W.H. Kan, W.R.M. Makahnouk and L.F. Nazar, *J. Mater. Chem*., **17**, 3248 (2007).
12. A.V. Murugan, T. Muraliganth and A. Manthiram, *J. Phys. Chem. C*, **112**, 14665 (2008).
13. F. Wang, J. Yang, Y. Nuli and J. Wang, *J. Power Sources*, **196**, 4806 (2011).
14. P.N. Poovizhi and S. Selladurai, *Ionics*, **17**, 13 (2011).
15. D. Wang, H. Buqa, M. Crouzet, G. Deghenghi, T. Drezen, I. Exnar, N.-H. Kwon, J.H. Miners, L. Poletto and M. Grätzel, *J. Power Sources*, **189**, 624 (2009).
16. C.M. Julien, P. Jozwiak and J. Garbarczyk, Proceedings of the International Workshop Advanced Techniques for Energy Sources Investigation and Testing, Sofia, Bulgaria, L4 (1) (2004).
17. Gangulibabu, D. Bhuvaneswari, N. Kalaiselvi, N. Jayaprakash and P. J. Periasamy, *Sol-Gel Sci. Technol*., **49**, 137 (2009).
18. A.V. Murugan, T. Muraliganth, P.J. Ferreira and A. Manthiram, *Inorg. Chem*., **48**, 946 (2009).